JACS
JOURNAL OF THE AMERICAN CHEMICAL SOCIETY

Communication

Mechanism of Alkyne Insertion of a Cationic Zirconocene Aryl Complex

Orson L. Sydora, Stefan M. Kilyanek, and Richard F. Jordan

J. Am. Chem. Soc., **2007**, 129 (43), 12952-12953• DOI: 10.1021/ja0760067 • Publication Date (Web): 04 October 2007

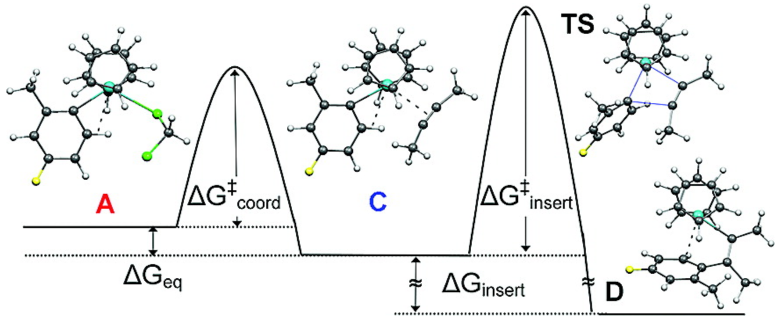

ACS Publications
High quality. High impact.

Journal of the American Chemical Society is published by the American Chemical Society. 1155 Sixteenth Street N.W., Washington, DC 20036

J|A|C|S
COMMUNICATIONS

Mechanism of Alkyne Insertion of a Cationic Zirconocene Aryl Complex

Orson L. Sydora, Stefan M. Kilyanek, and Richard F. Jordan*

Department of Chemistry, The University of Chicago, 5735 South Ellis Avenue, Chicago, Illinois, 60637

Received August 9, 2007; E-mail: rfjordan@uchicago.edu

Chain growth in metallocene-catalyzed alkene polymerization and alkyne oligomerization proceeds by coordination of substrate to the active d^0 L$_n$MR species followed by migratory insertion (eq 1).[1] The substrate adducts are transient species due to weak coordination and low insertion barriers and have not been directly observed.[2,3] Casey showed that Cp*$_2$YR alkyl complexes react with alkenes by fast reversible coordination followed by insertion.[4] The formation of Cp*$_2$Y(R)(alkene) species was inferred from NMR spectra of mixtures of Cp*$_2$YR and alkene, which contained one set of exchange-averaged alkene resonances shifted in the same direction from the free alkene positions as for chelated yttrium alkene complexes. Similarly, Erker showed that Cp′$_2$ZrCH$_2$CHCHCH$_2$B(C$_6$F$_5$)$_3$ (Cp′ = C$_5$H$_4$Me) and related betaine species react with alkenes by fast reversible coordination followed by insertion; however, again the intermediate adducts were not observed.[5] Here we report a Cp$_2$Zr(aryl)$^+$ system for which alkyne binding and insertion can be observed and quantified, enabling a description of the energy profile for the overall reaction.

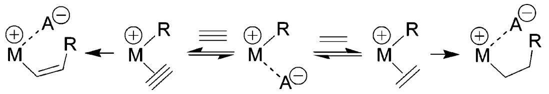

(1)

We reported that d^0 (C$_5$H$_4$R)$_2$Zr(C$_6$F$_5$)$^+$ (R = H, Me) species react with H$_2$C═CHCH$_2$SiMe$_3$ and HC≡CCH$_2$SiMe$_3$ to form (C$_5$H$_4$R)$_2$Zr(C$_6$F$_5$)(substrate)$^+$ adducts.[6] These species are stabilized by the β-Si effect and the low nucleophilicity of the C$_6$F$_5$ group and do not undergo insertion at temperatures up to 22 °C. These results suggested that modification of the aryl group and substrate might give species that form observable substrate adducts that are more reactive for insertion.

The complex [Cp$_2$Zr(4-F-*o*-tolyl)][B(C$_6$F$_5$)$_4$] (**1**, Cp = C$_5$H$_5$) was synthesized by the reaction of a 1/1 mixture of Cp$_2$Zr(4-F-*o*-tolyl)$_2$ and Cp$_2$ZrMe$_2$ with 2 equiv of [Ph$_3$C][B(C$_6$F$_5$)$_4$] at room temperature in the dark (eq 2).[7] This reaction proceeds by successive methyl abstraction and aryl exchange steps. In chlorocarbon solvents, **1** forms Cp$_2$Zr(4-F-*o*-tolyl)(RCl)$^+$ solvent adducts which contain β-H−Zr agostic interactions involving the aryl ortho C−H bond. DFT calculations for Cp$_2$Zr(4-F-*o*-tolyl)(CD$_2$Cl$_2$)$^+$ (**A**) show that the "endo" isomer in which the β-agostic interaction occupies the central coordination site is 6 kcal/mol more stable than the "exo" isomer in which the β-agostic interaction occupies a lateral site.

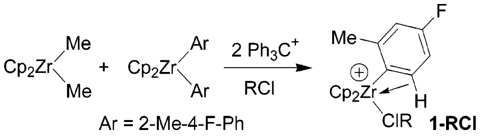

(2)

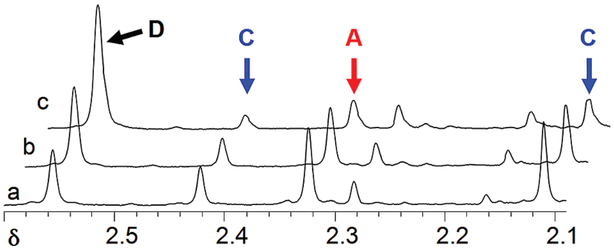

Figure 1. ^{1}H NMR spectra (CD$_2$Cl$_2$, −85 °C, Me region) of the reaction of Cp$_2$Zr(4-F-*o*-tolyl)(CD$_2$Cl$_2$)$^+$ (**A**) and excess 2-butyne, obtained immediately (a), 25 min (b), and 80 min (c) after thermal equilibration. Resonances of **A**, Cp$_2$Zr(4-F-*o*-tolyl)(2-butyne)$^+$ (**C**), and Cp$_2$Zr{CMe═CMe(4-F-*o*-tolyl)}$^+$ (**D**) are indicated (see text for assignments). The δ 2.16 peak is from Cp$_2$Zr(CMe═CMeCH$_2$C≡C*Me*)$^+$ formed by a minor C−H activation pathway. The δ 2.28 peak is from *m*-F-toluene formed in the synthesis of **A** and the C−H activation pathway.

The reaction of **A** with 2-butyne (**B**) was studied by low-temperature NMR and DFT calculations (BP86/LANL2DZ,6-31G*). A CD$_2$Cl$_2$ solution of **1** and excess 2-butyne was prepared at low temperature, transferred to a precooled NMR probe at −85 °C, thermally equilibrated, and monitored by NMR. Initially following the equilibration period, a mixture of **A**, the 2-butyne adduct Cp$_2$Zr(4-F-*o*-tolyl)(2-butyne)$^+$ (**C**), and the insertion product Cp$_2$Zr{CMe═CMe(4-F-*o*-tolyl)}$^+$ (**D**) was observed (eq 3). After 2 h, the formation of **D** was 90% complete. Complex **D** is thermally unstable and was not isolated.

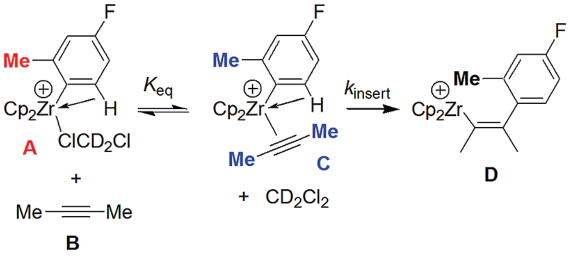

(3)

The methyl region of the ^{1}H NMR spectra of a reacting mixture of **A** and **B** is shown in Figure 1. The *o*-Me resonance of **A** appears at δ 2.32. The key resonances for **C** are the *o*-Me signal at δ 2.42 and the 2-butyne signal at δ 2.12, which is similar to that for Cp′$_2$Zr(O^{t}Bu)(2-butyne)$^+$ (δ 2.03).[2a] The presence of a single 2-butyne resonance for **C** indicates that 2-butyne rotation is fast on the NMR time scale, as observed for Cp′$_2$Zr(O^{t}Bu)(2-butyne)$^+$ and other d^0-metal alkyne complexes. The *o*-H resonance for **C** appears at high field (δ 5.98) indicative of an agostic interaction as in **A**. The DFT structure of **C** (Figure 2) contains a symmetrically bound alkyne (Zr−C = 2.85 Å) and an agostic *o*-C−H unit (Zr−H = 2.48 Å). The ^{1}H spectrum of **D** contains two Cp resonances indicating that the Cp rings are inequivalent, and two low field aryl resonances (δ 7.80, 7.51). The DFT structure of **D** contains close Zr−aryl contacts which may explain these features (Zr−C6, 2.56; Zr−H6, 2.65; Zr−C1, 2.92 Å). The *o*-Me signal of **D** appears at δ 2.56. Quenching **D** with MeOD gives DMeC═CMe(4-F-*o*-tolyl).

Several observations provide insight to the mechanism of eq 3. First, when 2-butyne (**B**) is present in >10 fold excess relative to **A**, the ratio [**A**]/[**C**] is constant throughout the reaction. This result

10.1021/ja0760067 CCC: $37.00 © 2007 American Chemical Society

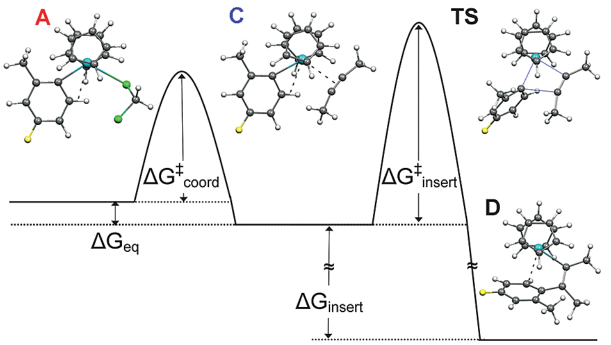

Figure 2. Free energy profile for conversion of **A** to **D** at −85 °C. Experimental ΔG and $\Delta G^{\ddagger}$ values (kcal/mol) are: $\Delta G_{\text{eq}} = -1.2$; $\Delta G^{\ddagger}_{\text{coord}}$ = ca. 10.6 to 11.5; $\Delta G^{\ddagger}_{\text{insert}} = 13.6$. $\Delta G_{\text{insert}} = -29.3$ kcal/mol (DFT).

implies that the exchange of bound and free alkyne (which is slow on the NMR time scale) is much faster than alkyne insertion. Second, the disappearance of the total of **A** and **C** in eq 3 obeys first-order kinetics. These results are consistent with a pre-equilibrium kinetic system, for which the rate law is given by eqs 4−6, where $K_{\text{eq}} = [\mathbf{C}][\mathbf{A}]^{-1}[\mathbf{B}]^{-1}$ is the equilibrium constant for alkyne binding,[8] k_{obs} is the first-order rate constant for the disappearance of the total of **A** and **C**, and k_{insert} is the rate constant for the insertion step. k_{obs} equals k_{insert} scaled by the fraction of metallocene that is in the reactive form ([**C**]/{[**A**] + [**C**]}; eq 5).

$$\text{rate} = \frac{\mathrm{d}([\mathbf{A}] + [\mathbf{C}])}{\mathrm{d}t} = -k_{\text{obs}}([\mathbf{A}] + [\mathbf{C}]) \qquad (4)$$

$$k_{\text{obs}} = \frac{K_{\text{eq}}[\mathbf{B}]k_{\text{insert}}}{K_{\text{eq}}[\mathbf{B}] + 1} = \frac{[\mathbf{C}]k_{\text{insert}}}{[\mathbf{A}] + [\mathbf{C}]} \qquad (5)$$

$$\ln\left(\frac{[\mathbf{A}] + [\mathbf{C}]}{[\mathbf{A}]_0 + [\mathbf{C}]_0}\right) = -k_{\text{obs}}t \qquad (6)$$

The alkyne binding constant determined by NMR integration is $K_{\text{eq}} = 1.4(1)$ M^{-1} at −85 °C, which, when solvent is taken into account, corresponds to $\Delta G_{\text{eq}} = -1.2$ kcal/mol.[8] The ΔG_{eq} estimated by DFT is −1.69 kcal/mol. This K_{eq} value is lower than that for 2-butyne coordination to $\text{Cp}'_2\text{Zr}(\text{O}^t\text{Bu})^+$ ($K_{\text{eq}} = 60$ M^{-1}, −85 °C, CD_2Cl_2).[2a]

The k_{obs} value ($2.1(2) \times 10^{-4}$ s^{-1}) was obtained by fitting the concentration versus time data to eq 6. The rate constant for insertion of **C** determined from K_{eq} and k_{obs} is $k_{\text{insert}} = 6.3(8) \times 10^{-4}$ s^{-1}, which corresponds to an insertion barrier of $\Delta G^{\ddagger}_{\text{insert}} = 13.5(4)$ kcal/mol. The $\Delta G^{\ddagger}_{\text{insert}}$ determined by DFT is 13.6 kcal/mol.

The barrier to alkyne coordination/decoordination was not determined. However, the absence of exchange line broadening in the NMR spectra of **A** and **C**, and the fact that the equilibrium between **A** and **C** is maintained throughout the reaction to produce **D**, imply that the barrier to conversion of **A** to **C** is between ca. 10.6−11.5 kcal/mol.[9] For comparison, the barrier to coordination of 2-butyne to $\text{Cp}'_2\text{Zr}(\text{O}^t\text{Bu})(\text{CD}_2\text{Cl}_2)^+$ (CD_2Cl_2, −85 °C) is 10.5 kcal/mol.[2a]

A free energy diagram based on these results is given in Figure 2. In the calculated insertion transition state (**TS**), the aryl ring is rotated 72° out of the metallocene bonding plane, which breaks the agostic interaction and brings the *o*-Me group close to the Cp rings. These effects contribute to the large insertion barrier. The Zr−C_{ipso} (2.34 Å) and C≡C (1.26 Å) distances are only slightly lengthened from the corresponding distances in **C** (2.23, 1.24 Å). The 2-butyne is bound unsymmetrically (Zr−C_{alkyne} = 2.41, 2.78 Å). These results are consistent with an early transition state similar to that found for the insertion of acetylene into $\text{Cp}_2\text{ZrCH}_3^+$.[10] NBO analysis of the insertion transition state shows significant overlap between the Zr−C σ bond and an alkyne π^* orbital, but nearly no overlap between the C_{ipso} p orbital and the alkyne π^* orbitals. In addition, NBO analysis reveals an aryl−Zr interaction involving overlap of the C_{ipso} p orbital with a Zr acceptor orbital. This interaction is analogous to the α-agostic interactions in alkene insertion transition states for d^0 metal alkyls.[11]

This work provides a quantitative picture of alkyne insertion in a $\text{Cp}_2\text{Zr}(\text{aryl})^+$ system. Alkyne insertion proceeds by reversible alkyne binding and rate-limiting insertion. Observation of the alkyne adduct is possible because the insertion barrier is high, owing to the presence of an agostic interaction that stabilizes the alkyne adduct and steric crowding between the aryl *o*-Me group and the Cp rings that destabilizes the insertion transition state. This approach may provide an opportunity to probe how the properties of the Cp_2M unit influence alkyne binding and insertion in $\text{Cp}_2\text{M}(\text{aryl})^+$ species.

Acknowledgment. This work was supported by the National Science Foundation (Grant CHE-0516950). We acknowledge the Burroughs Welcome Fund Interfaces Cross-Disciplinary Training Program for partial support of the computer cluster.

Supporting Information Available: Experimental and computational details. This material is available free of charge via the Internet at http://pubs.acs.org.

References

(1) (a) Resconi, L.; Cavallo, L.; Fait, A.; Piemontesi, F. *Chem. Rev.* **2000**, *100*, 1253. (b) Grubbs, R. H.; Coates, G. W. *Acc. Chem. Res.* **1996**, *29*, 85. (c) Horton, A. D. *Chem. Commun.* **1992**, 185. (d) den Haan, K. H.; Wielstra, Y.; Teuben, J. H. *Organometallics* **1987**, *6*, 2053. (e) Heeres, H. J.; Teuben, J. H. *Organometallics* **1991**, *10*, 1980. (f) Yoshida, M.; Jordan, R. F. *Organometallics* **1997**, *16*, 4508.

(2) For models see: (a) Stoebenau, E. J., III; Jordan, R. F. *Organometallics* **2006**, *25*, 3379. (b) Stoebenau, E. J., III; Jordan, R. F. *J. Am. Chem. Soc.* **2006**, *128*, 8162. (c) Witte, P. T.; Meetsma, A.; Hessen, B.; Budzelaar, P. H. M. *J. Am. Chem. Soc.* **1997**, *119*, 10561. (d) Humphries, M. J.; Douthwaite, R. E.; Green, M. L. H. *J. Chem. Soc., Dalton Trans.* **2000**, 2952. (e) Curtis, M. A.; Finn, M. G.; Grimes, R. N. *J. Organomet. Chem.* **1998**, *550*, 469. (f) Brandow, C. G.; Bercaw, J. E.; Mendiratta, A. *Organometallics* **2001**, *20*, 4253. (g) Martinez, G.; Royo, P. *Organometallics* **2005**, *24*, 4782. (h) Casey, C. P.; Klein, J. F.; Fagan, M. A. *J. Am. Chem. Soc.* **2000**, *122*, 4320. (i) Bonazza, A.; Cumurati, I.; Guidotti, S.; Mascellari, N.; Resconi, L. *Macromol. Chem. Phys.* **2004**, *205*, 319.

(3) Computational studies: (a) Yang, S. Y.; Ziegler, T. *Organometallics* **2006**, *25*, 887. (b) Landis, C. R.; Rosaaen, K. A.; Uddin, J. *J. Am. Chem. Soc.* **2002**, *124*, 12062. (c) Borrelli, M.; Busico, V.; Cipullo, R.; Ronca, S.; Budzelaar, P. H. M. *Macromolecules* **2002**, *35*, 2835.

(4) Casey, C. P.; Tunge, J. A.; Lee, T.-Y.; Fagan, M. A. *J. Am. Chem. Soc.* **2003**, *125*, 2641.

(5) Dahlmann, M.; Erker, G.; Bergander, K. *J. Am. Chem. Soc.* **2000**, *122*, 7986.

(6) Stoebenau, E. J., III; Jordan, R. F. *J. Am. Chem. Soc.* **2006**, *128*, 8638.

(7) Sydora, O. L.; Kilyanek, S. M.; Jordan, R. F. *Organometallics* **2007**, *26*, 4746.

(8) If solvent is included, the equilibrium constant is $K'_{\text{eq}} = [\text{C}][\text{solvent}][\text{A}]^{-1}[\text{B}]^{-1} = 21.8$, and $k_{\text{obs}} = K'_{\text{eq}}[\mathbf{B}]k_{\text{insert}}\{K'_{\text{eq}}[\mathbf{B}] + [\text{solvent}]\}^{-1}$. Since $K'_{\text{eq}} = K_{\text{eq}}$[solvent], this expression reduces to eq 5. ΔG_{eq} is based on K'_{eq}.

(9) The excess line width of **A** and **C** due to exchange is below the detection limit (ca. 0.5 Hz) and the formation of **A** from **C** is assumed to be >10 times faster than the conversion of **C** to **D**.

(10) Hyla-Kryspin, I.; Gleiter, R. *J. Mol. Catal. A: Chem.* **2000**, *160*, 115.

(11) (a) Leclerc, M. K.; Brintzinger, H. H. *J. Am. Chem. Soc.* **1995**, *117*, 1651. (b) Krauledat, H.; Brintzinger, H. H. *Angew. Chem., Int. Ed. Eng.* **1990**, *29*, 1412. (c) Piers, W. E.; Bercaw, J. E. *J. Am. Chem. Soc.* **1990**, *112*, 9406. (d) Chirik, P. J.; Dalleska, N. F.; Henling, L. M.; Bercaw, J. E. *Organometallics* **2005**, *24*, 2789.

JA0760067